Available online at www.sciencedirect.com
SCIENCE DIRECT®
Optics Communications 259 (2006) 765–771
OPTICS COMMUNICATIONS
www.elsevier.com/locate/optcom

Quantum interference effects in a multi-driven transition $F_g = 3 \leftrightarrow F_e = 2$

Dong Yabin, Zhang Junxiang *, Wang Haihong, Gao Jiangrui

State Key Laboratory of Quantum Optics and Quantum Optics Devices, Institute of Opto-Electronics, Shanxi University, 36 Wucheng Road, Taiyuan 030006, People's Republic of China

Received 9 June 2005; received in revised form 22 September 2005; accepted 22 September 2005

Abstract

We calculated and studied the quantum coherence effects of a degenerate transition $F_g = 3 \leftrightarrow F_e = 2$ system interacting with a weak linearly polarized (with $\sigma_\pm$ components) probe light and a strong linearly polarized (with $\sigma_\pm$ components) coupling field. Due to the competition between the drive Rabi frequency and the Zeeman splitting, electromagnetically induced transparency (EIT) and electromagnetically induced absorption (EIA) are appeared at the different values of applied magnetic field in both cases that the Zeeman splitting of excited state Δe is smaller than the Zeeman splitting of ground state Δg (i.e., $\Delta e < \Delta g$) and $\Delta e > \Delta g$. It is shown that the resonance is broader and contrasts are higher for $\Delta e < \Delta g$ than that for $\Delta e > \Delta g$ at the same Rabi frequencies of probe and coupling fields.
© 2005 Elsevier B.V. All rights reserved.

PACS: 42.50.Gy; 32.80.Qk

Keywords: Quantum coherence; Degenerate two-level system; Zeeman splitting

1. Introduction

Quantum coherences and interferences in atomic systems have led to a large number of important effects such as electromagnetically induced transparency (EIT) [1], coherent population trapping (CPT) [2], lasing without inversion (LWI) [3], and refractive index enhancement [4]. It was found that these effects have potential applications in quantum information system, for examples, storage of quantum information in a coherent media [5], quantum computation [4], quantum logic gate [6], quantum switches [7] and quantum interferometric optical lithography [8]. These phenomena have been widely studied in typical Λ-type and V-type three-level atomic systems. However, actual energy levels in atoms, molecules and solids are degenerate. A substantial enhancement of the absorption of a probe laser could occur when the drive laser is applied to a quasi-degenerate two-level atomic system forming a N-type scheme [9]. Akulshin's group [10–13] extensively studied the effects in atomic Rb vapor both experimentally and theoretically. They summarized that the requirements of enhancement of absorption induced by coherent radiation fields in an atomic system are as follows: (1) the ground state must be degenerate so that the coherence time between Zeeman sublevels is longer than that of the spontaneous decay from the upper level to the lower one in order to build up the atomic coherence of low frequency; (2) $0 < F_g < F_e$ (F_g and F_e are the total angular moments of the ground and the excited levels, respectively) for not forming CPT in the ground state; (3) the system must be closed. Goren et al. [14] distinguish two different

* Corresponding author. Tel.: +863517018240; fax: +863517011500.
E-mail address: zhangjxparis@yahoo.com (Z. Junxiang).

0030-4018/$ - see front matter © 2005 Elsevier B.V. All rights reserved.
doi:10.1016/j.optcom.2005.09.055

kinds of EIA: one is due to the transfer of coherence (TOC) between the excited and ground states via spontaneous decay. The other can occur when the collision transfer of population (TOP) from the ground state to a reservoir is greater than that from the excited state. Ying Gu et al. theoretically studied the transitions $F_e = 0 \leftrightarrow F_g = 1$, $F_e = 1 \leftrightarrow F_g = 0$ and $F_e = 1 \leftrightarrow F_g = 2$ [15–17], and concluded that EIT and EIA are obtained due to the competition between the driver Rabi frequency and the Zeeman splitting. Chengpu Liu et al. reported that the transitions from EIT to EIA in the Λ system of near degenerate levels is due to a spontaneously generated coherence, i.e., relative phase of the two applied fields [18]. The experimental showing of the transfer of EIT into EIA for the case of $F_e < F_g$ was given by Soo Kyoung Kim et al., recently [19].

Most schemes used to explain these effects were concentrated on Λ-type, V-type three-level, N-type four-level or simple degenerate two level atomic systems. With the investigation of multicoherence experimentally and theoretically, many newer and more complex quantum coherence effects are related to the interactions between multi-field and multilevel systems. Possessing two transparency points and three absorption peaks, double dark states resonance and double EIT have attracted great interest in dipole quantum well laser and quantum computer [20]. In this paper, we use optical Bloch equations to study the quantum coherence effects induced by the competition between the coupling field and the Zeeman splitting, when two independent linearly polarized coherent fields interact on the transition $F_g = 3 \leftrightarrow F_e = 2$ employed as a degenerate two-level system, which can be realized in the hyperfine transition between the states $6^2S_{1/2}$ $(F = 3)$ and $6^2P_{3/2}$ $(F = 2)$ of Cs. Compared to the results in [17] in which EIA occurs in the case that the Zeeman splitting of excited state Δe is equal to or smaller than the Zeeman splitting of ground state Δg (i.e., $\Delta e \leqslant \Delta g$), the EIT and EIA in the system of transition $F_g = 3 \leftrightarrow F_e = 2$ are obtained in both cases of $\Delta e \leqslant \Delta g$ and $\Delta e > \Delta g$ due to the multicoherence induced by multilevel transitions. On the whole, the degenerate two-level atom system that Ying Gu group and other groups have studied are the one that the driven field is the linearly polarized light interacting on the transition $M_{F_g} \leftrightarrow M_{F_e} = M_{F_g}$ and the probe field is the other linearly polarized light which has left circular polarized and right circular polarized components interacting on the transition $M_{F_g} \leftrightarrow M_{F_e} = M_{F_g} \pm 1$. In this paper, however, not only the probe field but also the driven field are the linearly polarized light which include left circular polarized and right circular polarized components interacting on the transition $M_{F_g} \leftrightarrow M_{F_e} = M_{F_g} \pm 1$. So both the driven field and the probe field interact on all sub-levels of ground states while the driven field or the probe field doesn't interact on some sub-levels of ground states in original patterns. It results in that the population distribution on the sub-levels in our model is different from the original patterns. Therefore, the different phenomena will appear. Not considering Doppler effects, this work is relevant for cold Cs atoms.

2. Optical Bloch equations

Let us consider the transition $F_g = 3 \leftrightarrow F_e = 2$, as shown in Fig. 1, driven and probed by two linearly lights with frequency ω_c and ω_p, respectively, which co-propagate along the vector direction of static magnetic field. According to the Zeeman effect, both fields have two equal left and right polarized components $\sigma_\pm$ as long as the polarizations of two fields are orthogonal to the vector direction of static magnetic field. Whatever the polarizations of two fields are orthogonal or parallel to each other. Here $\sigma_\pm$ light interacts with the transition $M_{F_e} = i \leftrightarrow M_{F_g} = i \pm 1$ with $i = 0, \pm 1, \pm 2$. The excited states are expressed as $|e_{-2}\rangle$, $|e_{-1}\rangle$, $|e_0\rangle$, $|e_1\rangle$ and $|e_2\rangle$, while the ground states are $|g_{-3}\rangle$, $|g_{-2}\rangle$, $|g_{-1}\rangle$, $|g_0\rangle$, $|g_1\rangle$, $|g_2\rangle$ and $|g_3\rangle$. Only the decay of the atomic levels due to spontaneous emission ($\Gamma_{eg} = \Gamma$) and collisions ($\Gamma_{ee} = \Gamma_{gg} = \Gamma_0$) that result in dephasing of the coherences and exchange of population between the Zeeman sublevels are considered [15–17]. In rotating-wave approximation, the temporal evolution of the density matrix of the system is governed by

$$\dot{\rho}_{e_i g_j} = \frac{\mathrm{i}}{\hbar}\left[\sum_k (V_{e_i g_k}\rho_{g_k g_j} - \rho_{e_i e_k} V_{e_k g_j})\right] - (\mathrm{i}\omega_{e_i g_j} + \gamma_{eg})\rho_{e_i g_j}, \tag{1}$$

$$\dot{\rho}_{e_i e_i} = \frac{\mathrm{i}}{\hbar}\sum_k (V_{e_i g_k}\rho_{g_k e_i} - \rho_{e_i g_k} V_{g_k e_i}) - (7\Gamma + 4\Gamma_0)\rho_{e_i e_i} + \Gamma_0 \sum_{j \neq i} \rho_{e_j e_j}, \tag{2}$$

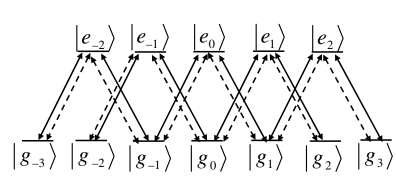

Fig. 1. Zeeman sub-level structure for a transition $F_g = 3 \leftrightarrow F_e = 2$ and configuration of laser field. The drive and probe fields are both coherent lights which have circularly polarized components $\sigma_\pm$. Solid lines represent the drive field, and dashed line is for probe field.

$$\dot{\rho}_{e_ie_j} = \frac{\mathrm{i}}{\hbar}\sum_k (V_{e_ig_k}\rho_{g_ke_j} - \rho_{e_ig_k}V_{g_ke_j}) - (\mathrm{i}\omega_{e_ie_j} + \gamma_{ee})\rho_{e_ie_j}, \tag{3}$$

$$\dot{\rho}_{g_ig_i} = \frac{\mathrm{i}}{\hbar}\sum_k (V_{g_ie_k}\rho_{e_kg_i} - \rho_{g_ie_k}V_{e_kg_i}) - 6\Gamma_0\rho_{g_ig_i} + \Gamma\sum_{i=-2}^{2}\rho_{e_ie_i} + \Gamma_0\sum_{j\neq i}\rho_{g_jg_j}, \tag{4}$$

$$\dot{\rho}_{g_ig_j} = \frac{\mathrm{i}}{\hbar}\sum_k (V_{g_ie_k}\rho_{e_kg_j} - \rho_{g_ie_k}V_{e_kg_j}) - (\mathrm{i}\omega_{g_ig_j} + \gamma_{gg})\rho_{g_ig_j}, \tag{5}$$

where $V_{e_ig_j}$ represents the interacting energy for the $|e_i\rangle \to |g_j\rangle$ transition; $\omega_{e_ie_j} = \omega_{e_i} - \omega_{e_j}$ and $\omega_{g_ig_j} = \omega_{g_i} - \omega_{g_j}$ denote the Zeeman splitting of excited state and ground states, respectively; $\omega_{k_ik_j} = g_k\mu_b B/\hbar$ $(i = j \pm 1)$ is the Raman detuning induced by the magnetic field of strength B, where g_k ($k = e$ or g) is Lande factor, μ_b is the Bohr magnetron; $\omega_{e_ig_j} = \omega_{e_i} - \omega_{g_j}$ is transition frequency between excited and ground degenerate levels; $\gamma_{ee} = 7\Gamma + 4\Gamma_0$, $\gamma_{eg} = \frac{1}{2}(7\Gamma + 10\Gamma_0)$, and $\gamma_{gg} = 6\Gamma_0$ are decay rates corresponding to different transitions. Ignoring the effect of spatial variation of the field amplitude, the interaction energy for the transition from level g_j to e_i is written as $V_{e_ig_j} = \hbar V_{e_ig_j}(\omega_c)\mathrm{e}^{-\mathrm{i}\omega_c t} + \hbar V_{e_ig_j}(\omega_p)\mathrm{e}^{-\mathrm{i}\omega_p t}$ with $i = 0, \pm1, \pm2$, $j = i \pm 1$. Here, the magnitudes of $2V_{e_ig_j}(\omega_p) = \mu_{e_ig_j}E_p/2^{1/2}\hbar$ and $2V_{e_ig_j}(\omega_c) = \mu_{e_ig_j}E_c/2^{1/2}\hbar$ are the Rabi frequency of probe and drive fields, respectively. The dipole moments of transitions are taken as $\mu_{e_{-2}g_{-3}} = \mu_{e_2g_3} = -\sqrt{\frac{5}{14}}\mu$, $\mu_{e_{-2}g_{-1}} = \mu_{e_2g_1} = -\sqrt{\frac{5}{21}}\mu$, $\mu_{e_{-1}g_{-2}} = \mu_{e_1g_2} = -\sqrt{\frac{1}{42}}\mu$, $\mu_{e_{-1}g_0} = \mu_{e_1g_0} = -\sqrt{\frac{1}{7}}\mu$ and $\mu_{e_0g_{-1}} = \mu_{e_0g_1} = -\sqrt{\frac{1}{14}}\mu$ for Cs D_2 line data [21].

Considering the condition that the drive light is much stronger than probe light, we treat drive field to all orders in its Rabi frequency and meanwhile probe field to first order, then $\rho_{e_ig_j}$ oscillates at three frequencies [22,23]: the pump frequency ω_c, the probe frequency ω_p and the four-wave mixing frequency $2\omega_c - \omega_p$. We therefore express $\rho_{e_ig_j}$ in terms of its Fourier amplitudes as:

$$\rho_{e_ig_j} = \rho_{e_ig_j}(\omega_c)\mathrm{e}^{-\mathrm{i}\omega_c t} + \rho_{e_ig_j}(\omega_p)\mathrm{e}^{-\mathrm{i}\omega_p t} + \rho_{e_ig_j}(2\omega_c - \omega_p)\mathrm{e}^{-\mathrm{i}(2\omega_c - \omega_p)t}. \tag{6}$$

Similarly, the populations and coherences within the same hyperfine level can be written as

$$\rho_{k_ik_j} = \rho^{\mathrm{dc}}_{k_ik_j} + \rho_{k_ik_j}(\omega_c - \omega_p)\mathrm{e}^{-\mathrm{i}(\omega_c - \omega_p)t} + \rho_{k_ik_j}(\omega_p - \omega_c)\mathrm{e}^{-\mathrm{i}(\omega_p - \omega_c)t}, \tag{7}$$

where $\rho_{k_ik_j}(\omega_c - \omega_p)\mathrm{e}^{-\mathrm{i}(\omega_c - \omega_p)t}$ and $\rho_{k_ik_j}(\omega_p - \omega_c)\mathrm{e}^{-\mathrm{i}(\omega_p - \omega_c)t}$ are population and coherence oscillations at frequencies $\omega_c - \omega_p$ and $\omega_p - \omega_c$. In the steady state, we obtain a set of linear equations for the Fourier amplitudes:

$$\begin{aligned}\dot{\rho}_{e_ie_i}(\omega_p - \omega_c) = {} & [\mathrm{i}(\omega_p - \omega_c) - (7\Gamma + 4\Gamma_0)]\rho_{e_ie_i}(\omega_p - \omega_c) - \mathrm{i}\sum_k[\rho_{e_ig_k}(\omega_p)V_{g_ke_i}(-\omega_c) \\ & - V_{e_ig_k}(\omega_c)\rho_{g_ke_i}(\omega_p - 2\omega_c) - V_{e_ig_k}(\omega_p)\rho_{g_ke_i}(-\omega_c)] + \Gamma_0\sum_{j\neq i}\rho_{e_je_j}(\omega_p - \omega_c),\end{aligned} \tag{8}$$

$$\begin{aligned}\dot{\rho}_{e_ie_j}(\omega_p - \omega_c) = {} & [\mathrm{i}(\omega_p - \omega_c - \omega_{e_ie_j}) - \gamma_{ee}]\rho_{e_ie_j}(\omega_p - \omega_c) - \mathrm{i}\sum_k[\rho_{e_ig_k}(\omega_p)V_{g_ke_j}(-\omega_c) \\ & - V_{e_ig_k}(\omega_c)\rho_{g_ke_j}(\omega_p - 2\omega_c) - V_{e_ig_k}(\omega_p)\rho_{g_ke_j}(-\omega_c)],\end{aligned} \tag{9}$$

$$\begin{aligned}\dot{\rho}_{g_ig_i}(\omega_p - \omega_c) = {} & [\mathrm{i}(\omega_p - \omega_c) - 6\Gamma_0]\rho_{g_ig_i}(\omega_p - \omega_c) + \mathrm{i}\sum_k[\rho_{e_kg_i}(\omega_p)V_{g_ie_k}(-\omega_c) - V_{e_kg_i}(\omega_c)\rho_{g_ie_k}(\omega_p - 2\omega_c) \\ & - V_{e_kg_i}(\omega_p)\rho_{g_ie_k}(-\omega_c)] + \Gamma\sum_j\rho_{e_je_j}(\omega_p - \omega_c) + \Gamma_0\sum_{j\neq i}\rho_{g_jg_j}(\omega_p - \omega_c),\end{aligned} \tag{10}$$

$$\begin{aligned}\dot{\rho}_{g_ig_j}(\omega_p - \omega_c) = {} & [\mathrm{i}(\omega_p - \omega_c - \omega_{g_ig_j}) - \gamma_{gg}]\rho_{g_ig_j}(\omega_p - \omega_c) + \mathrm{i}\sum_k[\rho_{e_kg_j}(\omega_p)V_{g_ie_k}(-\omega_c) \\ & - V_{e_kg_j}(\omega_c)\rho_{g_ie_k}(\omega_p - 2\omega_c) - V_{e_kg_j}(\omega_p)\rho_{g_ie_k}(-\omega_c)],\end{aligned} \tag{11}$$

$$\begin{aligned}\dot{\rho}_{e_ig_j}(\omega_p) = {} & [\mathrm{i}(\omega_p - \omega_{e_ig_j}) - \gamma_{eg}]\rho_{e_ig_j}(\omega_p) - \mathrm{i}\left\{\sum_k[\rho^{\mathrm{dc}}_{e_ie_k}V_{e_kg_j}(\omega_p) - V_{e_ig_k}(\omega_p)\rho^{\mathrm{dc}}_{g_kg_j}]\right. \\ & \left. + \sum_k[\rho_{e_ie_k}(\omega_p - \omega_c)V_{e_kg_j}(\omega_c) - V_{e_ig_k}(\omega_c)\rho_{g_kg_j}(\omega_p - \omega_c)]\right\},\end{aligned} \tag{12}$$

$$\dot{\rho}_{e_ig_j}(2\omega_c - \omega_p) = [i(2\omega_c - \omega_p - \omega_{e_ig_j}) - \gamma_{eg}]\rho_{e_ig_j}(2\omega_c - \omega_p) - \mathrm{i}\left\{\sum_k[\rho_{e_ie_k}(\omega_c - \omega_p)V_{e_kg_j}(\omega_c) - V_{e_ig_k}(\omega_c)\rho_{g_kg_j}(\omega_c - \omega_p)]\right\}. \tag{13}$$

Since we are only interested in the steady-state results, we set the time derivatives of the Fourier amplitudes in Eqs. (8)–(13) equal to zero. When the system is closed, it satisfied the relation: $\sum_i \rho_{e_ie_i} + \sum_j \rho_{g_jg_j} = 1$ with $i = 0, \pm1, \pm2$ and $j = 0, \pm1, \pm2, \pm3$. And if the relation $\rho_{ij}(\omega_k) = \rho^*_{ij}(-\omega_k)$ is taken into account, these linear equations are readily solved.

The probe absorption is calculated from the imaginary part of the susceptibility $\chi(\omega_p)$. For transition $F_e = 2 \leftrightarrow F_g = 3$, we have:

$$\begin{aligned}\mathrm{Im}\chi(\omega_p) \propto \mathrm{Im}\{[&\mu_{e_{-2}g_{-3}}(\rho_{e_{-2}g_{-3}}(\omega_p) + \rho_{e_2g_3}(\omega_p)) + \mu_{e_{-2}g_{-1}}(\rho_{e_{-2}g_{-1}}(\omega_p) + \rho_{e_2g_1}(\omega_p)) + \mu_{e_{-1}g_{-2}}(\rho_{e_{-1}g_{-2}}(\omega_p) \\ &+ \rho_{e_1g_2}(\omega_p)) + \mu_{e_{-1}g_0}(\rho_{e_{-1}g_0}(\omega_p) + \rho_{e_1g_0}(\omega_p)) + \mu_{e_0g_{-1}}(\rho_{e_0g_{-1}}(\omega_p) + \rho_{e_0g_1}(\omega_p))]/(V_{e_0g_{-1}}/\gamma_{eg})\}. \qquad (14)\end{aligned}$$

3. Numerical calculation results and discussions

To model the quantum coherence effects of transition $F_e = 2 \leftrightarrow F_g = 3$ shown in Fig. 1, we first define the parameters in the Bloch equations. If γ_{eg} is normalized to 1.0, then we have $\Gamma = 0.282$, $\Gamma_0 = 0.01\Gamma = 0.00282$, $\gamma_{ee} = 7\Gamma + 4\Gamma_0 = 1.983$ and $\gamma_{gg} = 6\Gamma_0 = 0.01692$. The frequency detuning of drive light is $\Delta = \omega_c - \omega_{e_0g_0}$, and the frequency detuning of probe is $\delta = \omega_p - \omega_{e_0g_0}$. For simplicity, we have $V_{e_ig_j}(\omega_p)$ and $V_{e_ig_j}(\omega_c)$ to be real.

We first consider the case of degenerate two-level atomic system (i.e., $B = 0$ or $\Delta e = \Delta g = 0$). It can be treated as a superposition of 10 Λ-type sub-systems ($M_{F_g} = i \pm 1 \leftrightarrow M_{F_e} = i \leftrightarrow M_{F_g} = i \mp 1$ with $i = 0, \pm1, \pm2$) and 10 pure two-level ($M_{F_g} = i - 1 \leftrightarrow M_{F_e} = i \leftrightarrow M_{F_g} = i - 1$ and $M_{F_g} = i + 1 \leftrightarrow M_{F_e} = i \leftrightarrow M_{F_g} = i + 1$) sub-systems.

The absorption of the probe field as a function of the frequency detuning of probe field for different Rabi frequency of the drive light is shown in Fig. 2. When V_c is taken to be 0.5, EIT appears (see Fig. 2(a)) in the center of the spectrum. Here $V_c = E_c/2\sqrt{2}$ and $V_p = E_p/2\sqrt{2}$. When V_c is increased to be 1.5, three transparency peaks emerge (see Fig. 2(b)). On further increasing V_c, the spectrum (see Fig. 3) is similar to the typical Mollow absorption spectrum (MAS) observed by Wu et al. [24]. If the drive field has detuning Δ, the transparent point of EIT is shifted with the detuning (see Fig. 4(a)). It is seen that with the detuning increasing, the transparent gets more like dispersion curve (see Fig. 4(b)).

When a magnetic field is applied, the degeneracy is broken and Zeeman splitting is non-zero. In this case, not only the coherence between the Zeeman splitting and drive field, but also the coherence among the Zeeman splittings belonging to different states, should be considered. Note that the Zeeman splitting Δe (or $\omega_{e_1e_0}$) of the excited state is normally not equal

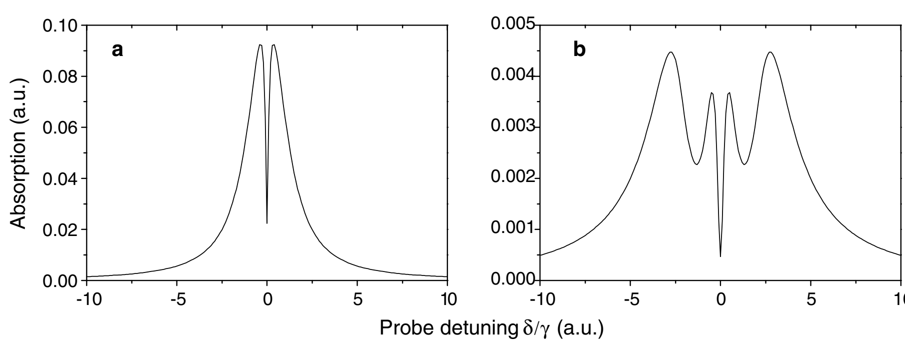

Fig. 2. The absorption of the probe field as a function of the frequency detuning of probe field for different Rabi frequency of the drive light in the case of degenerate two-level atom system (i.e., $B = 0$). (a) $V_c = 0.5$; (b) $V_c = 1.5$. Here $V_p = 0.01$, $\Gamma = 0.282$, $\Gamma_0 = 0.00282$, $\gamma_{ee} = 1.983$, $\gamma_{gg} = 0.01692$ and the frequency detuning of drive field Δ is zero.

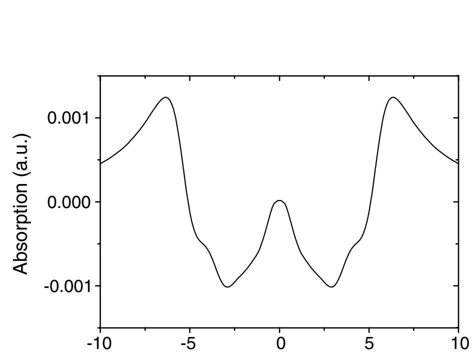

Fig. 3. The Mollow absorption spectrum of the degenerate two-level atomic system as a function of the frequency detuning of probe field at $V_c = 3.5$. Here $V_p = 0.01$, $\Gamma = 0.282$, $\Gamma_0 = 0.00282$, $\gamma_{ee} = 1.983$, $\gamma_{gg} = 0.01692$ and the frequency detuning of drive field Δ is zero.

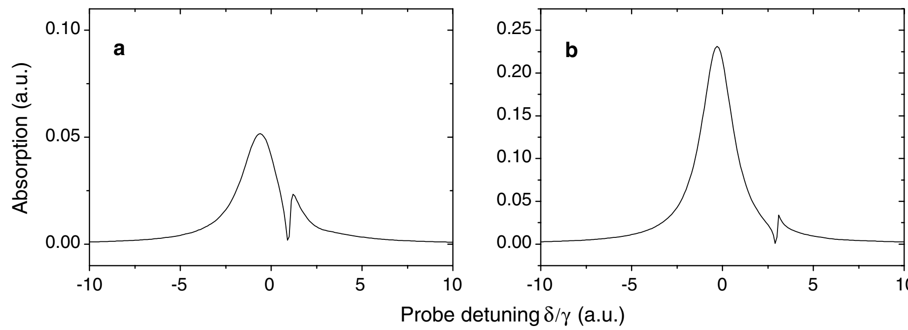

Fig. 4. Absorption of the degenerate two-level atomic system as a function of the frequency detuning of probe field with the frequency detuning of drive field Δ no zero: (a) $\Delta = 1$; (b) $\Delta = 1$. Here $V_p = 0.01$, $\Gamma = 0.282$, $\Gamma_0 = 0.00282$, $\gamma_{ee} = 1.983$, $\gamma_{gg} = 0.01692$.

to the splitting Δg (or $\omega_{g_1 g_0}$) of the ground state. In the following subsections, the absorption spectrums are discussed for $\Delta e > \Delta g$ and $\Delta e < \Delta g$, respectively.

3.1. The Zeeman splitting $\Delta e > \Delta g$

Fig. 5 shows the quantum multicoherence effects with the Zeeman splitting $\Delta e = 0.93 * B$, $\Delta g = 0.35 * B$ (here B is the intensity of magnetic field, CGS units), which corresponds to the actual Zeeman splitting of $6^2S_{1/2}$ $(F = 3)$ and $6^2P_{3/2}$ $(F = 2)$ states of Cs atoms.

As shown in Fig. 5(a) and (b), when the intensity of magnetic field B is increased from $B = 0.1$ to 0.4 (Zeeman splitting is also increasing, but it is small compared to V_c), the spectrum changes from EIT to EIA. On further increasing the intensity of magnetic field B, the absorption peak becomes wider (see Fig. 5(c)). If the intensity of magnetic field B becomes big compared to V_c as shown in Fig. 5(d), the spectrum at resonance turns into transparency again; three transparency windows and two absorption peaks are observed in this case.

3.2. The Zeeman splitting $\Delta e < \Delta g$

When we consider the case for $\Delta e < \Delta g$, which corresponds to the actual Zeeman splitting of $6^2S_{1/2}$ $(F = 4)$ and $6^2P_{3/2}$ $(F = 3)$ of Cs atoms (Here $\Delta e = 0.00056 * B$, $\Delta g = 0.35 * B$), the EIA effect induced by multicoherence is enhanced. As illustrated in Fig. 6(a) and (b), in which the parameters V_c, B are taken to be the same as we take in Fig. 5. It is obviously

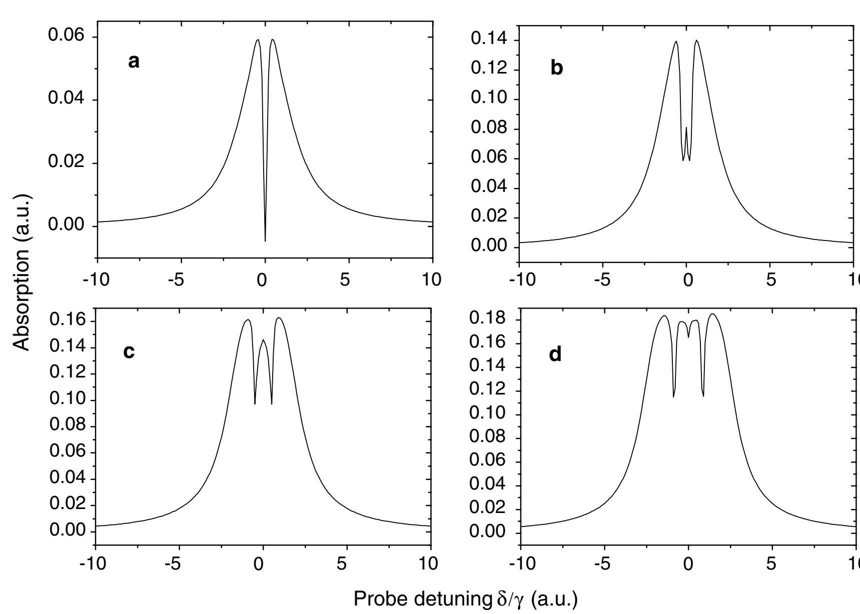

Fig. 5. The absorption of the probe field as a function of the frequency detuning of probe field for different Rabi frequency of the drive light with Zeeman splittings $\Delta e = 0.93 * B$ and $\Delta g = 0.35 * B$. (a) $B = 0.1$; (b) $B = 0.4$; (c) $B = 0.7$; (d) $B = 1.2$. Parameters: $V_c = 0.8$, $V_p = 0.01$, $\Gamma = 0.282$, $\Gamma_0 = 0.00282$, $\gamma_{ee} = 1.983$, $\gamma_{gg} = 0.01692$ and $\Delta = 0$.

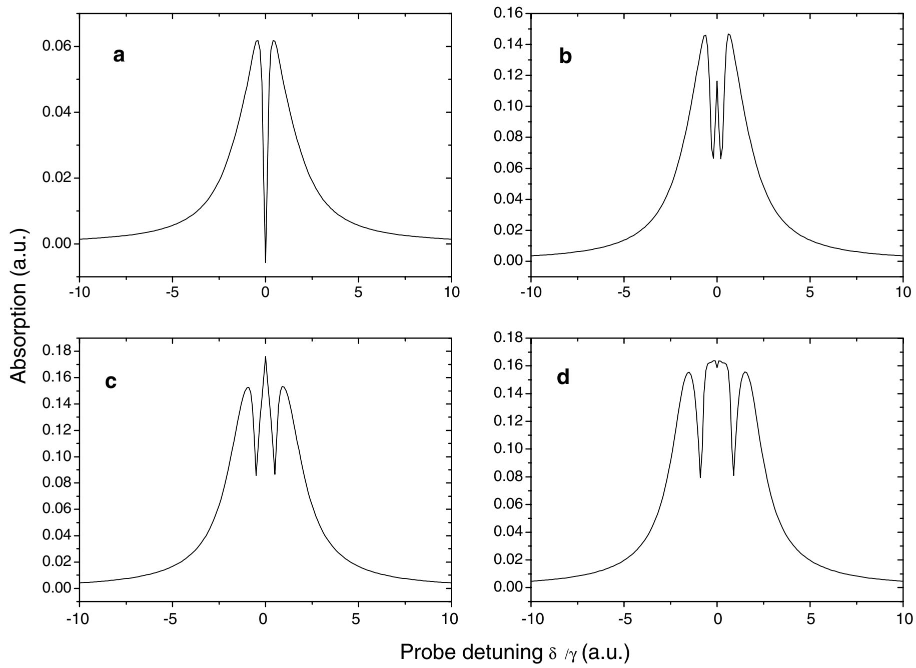

Fig. 6. The absorption of the probe field as a function of the frequency detuning of probe field for different Rabi frequency of the drive light with Zeeman splittings $\Delta e = 0.00056 * B$ and $\Delta g = 0.35 * B$. (a) $B = 0.1$; (b) $B = 0.4$; (c) $B = 0.7$; (d) $B = 1.2$. Parameters: $V_c = 0.8$, $V_p = 0.01$, $\Gamma = 0.282$, $\Gamma_0 = 0.00282$, $\gamma_{ee} = 1.983$, $\gamma_{gg} = 0.01692$ and $\Delta = 0$. It is seen that the EIA effects in (b) and (c) is clearly more prominent than that of (b) and (c) in Fig. 5.

seen that the absorption peaks in Fig. 6(b) and (c) are higher than that in Fig. 5(b) and (c). When B is further increased, the spectrum of EIA turns into transparency (see Fig. 6(d)), but it is smaller than that shown in Fig. 5(d).

It is noted that when we keep the Zeeman splitting of ground state Δg fixed, the EIA effects become stronger with the Δe decreasing. For the case of $\Delta e = \Delta g$, it is easy to deduce that the quantum coherence effects are between the cases of $\Delta e < \Delta g$ and $\Delta e > \Delta g$. Thus both the EIT and EIA can be obtained in this case.

4. Conclusions

Quantum coherence effects of Zeeman hyperfine splitting among two-level atomic system are studied when two independent linearly polarized coherent lasers interact on a degenerate two-level system, which is put in a static magnetic field. Both polarizations of coherent fields are orthogonal to the vector direction of static magnetic field and they both have two equal left and right polarized components $\sigma_\pm$ interact with the transition $M_{F_e} = i \leftrightarrow M_{F_g} = i \pm 1$ with $i = 0, \pm 1, \pm 2$. If the intensity of magnetic field is zero, i.e., no Zeeman splitting, the atomic system is degenerate, only EIT can be found. Increasing Rabi frequency of the pump field, three transparency windows emerges in the spectrum, and when the Rabi frequency of the pump field is further increased, we can find that the typical Mollow absorption spectrum appears. If a magnetic field is applied along the light transmission direction, the degeneracy is broken, thus the multicoherences are introduced, and both the EIT and EIA are obtained at the different values of magnetic field. It is also shown that the EIA are more marked under the condition of $\Delta e < \Delta g$ than that in $\Delta e > \Delta g$.

Acknowledgments

The work was supported by the National Natural Science Foundation of China (No. 60278010) and Shanxi Natural Science Foundation (No. 20041039). The authors thank Dr. Ying Gu for helpful discussions.

References

[1] K.J. Boller, A. Imamolu, S.E. Harris, Phys. Rev. Lett. 66 (1991) 2593.
[2] H.R. Gray, R.M. Whitley, C.R. Stroud Jr., Opt. Lett. 3 (1978) 218.
[3] S.E. Harris, Phys. Rev. Lett. 62 (1989) 1033.
[4] M.O. Scully, Phys. Rev. Lett. 67 (1991) 1855.
[5] D.F. Phillips, A. Fleischhauer, A. Mair, R.L. Walsworth, Phys. Rev. Lett. 86 (2001) 783.
[6] Q.A. Turchette, C.J. Hood, W. Lange, H. Mabuchi, H.J. Kimble, Phys. Rev. Lett. 75 (1995) 4710.

[7] S.E. Harris, Y. Yamamoto, Phys. Rev. Lett. 81 (1998) 3611.
[8] A.N. Boto, P. Kok, D.S. Abrams, S.L. Braunstein, C.P. Williams, J.P. Dowling, Phys. Rev. Lett. 85 (2000) 2733.
[9] A.V. Taichenachev, A.M. Tumaikin, V.I. Yudin, Phys. Rev. A 61 (1999) 011802.
[10] A.M. Akulshin, S. Barreiro, A. Lezama, Phys. Rev. A 57 (1998) 2996.
[11] A. Lezama, S. Barreiro, A.M. Akulshin, Phys. Rev. A 59 (1999) 4732.
[12] A. Lezama, S. Barreiro, A. Lipsich, A.M. Akulshin, Phys. Rev. A 61 (1999) 013801.
[13] A. Lipsich, S. Barreiro, A.M. Akulshin, A. Lezama, Phys. Rev. A 61 (2000) 053803.
[14] C. Goren, A.D. Wilson-Gordon, M. Rosenbluh, H. Friedmann, Phys. Rev. A 67 (2003) 033807.
[15] Ying Gu, Qingqing Sun, Qihuang Gong, Phys. Rev. A 67 (2003) 063809.
[16] Qingqing Sun, Ying Gu, Qihuang Gong, J. Mod. Opt. 51 (2004) 1899.
[17] Ying Gu, Qingqing Sun, Qihuang Gong, J. Phys. B 37 (2004) 1553.
[18] Cheng-pu Liu, Shang-qing Gong, Xi-jun Fan, Zhi-zhan Xu, Opt. Commun. 231 (2004) 289.
[19] Soo Kyoung Kim, Han Seb Moon, Kyoungdae Kim, Jung Bog Kim, Phys. Rev. A 68 (2003) 063813.
[20] T. Pellizzari, S.A. Gardiner, J.I. Cirac, P. Zoller, Phys. Rev. Lett. 75 (1995) 3788.
[21] Daniel A. Steck, 2003. Available from: <http://steck.us/alkalidata>.
[22] A.D. Wilson-Gordon, H. Friedmann, Opt. Lett. 8 (1983) 617.
[23] R.W. Boyd, M.G. Raymer, P. Narum, D.J. Harter, Phys. Rev. A 24 (1981) 411.
[24] F.Y. Wu, S. Ezekiel, M. Ducloy, B.R. Mollow, Phys. Rev. Lett. 38 (1977) 1077.